High Performance and Cost Effective ZCS Matrix Resonant Inverter for Total Active Surface Induction Heating Appliances

H. Sarnago, *Member, IEEE,* J.M. Burdio, *Senior Member*, *IEEE*, and O. Lucía, *Senior Member*, *IEEE*.

***Abstract*- Flexible cooking surfaces represent the most innovative and high-performance induction heating appliances nowadays. This paper presents a multiple-output resonant inverter for multi-coil systems featuring high efficiency and flexible output power control for modern induction heating appliances. By adopting a matrix structure, the number of controlled devices can be significantly reduced while a high control versatility is ensured. The proposed converter is firstly analyzed and, in order to prove the feasibility of the proposal, a multiple-output prototype is designed and implemented. The experimental results prove the correct converter operation and output power control with multiple induction heating loads, validating the proposed approach.**

***Keywords* – Induction heating, home appliances, resonant power conversion, inverters.**

I. Introduction

Induction heating (IH) has become the heating technology of choice in many industrial [1], domestic [2] and medical applications [3] due to its benefits in terms of efficiency cleanliness and performance, leading to a superior quality process [4]. Regardless the application, IH is based on applying an alternating magnetic field to an induction target to be heated. The design of the coil as well as the ac source, i.e. power converter, must be adapted to the characteristics of the desired process, including the target geometry and temperature distribution, among others.

Modern household appliances are intended to be high performance products presenting a balanced set of features including mainly efficiency and user performance, among others. To achieve these aims, power electronics play a key role enabling the design of highly efficient and performance products. Among the wide set of home appliances, induction heating (IH) cookers [4] are a relevant example where power electronics play a key role to implement such systems with relevant advantages in terms of efficiency, safety, cleanness, and fast heating.

Modern design trends for IH appliances are advancing towards the design of multi-coil systems (Fig. 1) that provide superior features compared with conventional units [2]. These systems provide unprecedented flexibility since any number of pots can be used, with any shape and in any position of the cooking surface. This provides an improved user performance which brings induction heating to a leading position in the household technology portfolio.

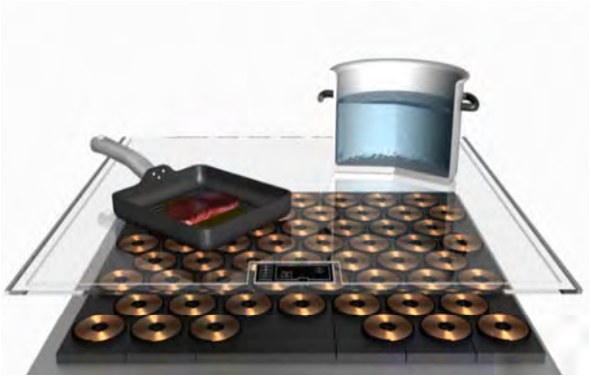

Fig. 1. Flexible IH appliance.

These appliances present several key challenges including the design of small induction coils with high coupling, the power converter as well as the complex control of a high number of loads. In particular, these appliances require the design of power converters able to supply a high number of coils in an efficient, versatile and cost-effective manner [5, 6] and complying with EMC standards [7].

The aim of this paper is therefore to propose a multiple-output ZCS resonant inverter that following a matrix approach [8] enables a cost-effective implementation while ensuring accurate output power control and efficient operation in a wide set of operating conditions. This proposal fulfills both requisites for multi-coil systems with superior performance and decreased power device count. The remainder of this paper is organized as follows. Section II reviews the power converter topologies proposed for flexible IH cooking surfaces. Section III presents the proposed multiple-output ZCS resonant inverter, focusing on the topology and its equivalent circuits, as well as the main modulation strategies. Section IV shows the main experimental results proving the feasibility of this proposal and Section V presents a comparative analysis of the proposed approach compared with state-of-the-art solutions. Finally, Section VI draws the main conclusions of this paper.

This work was partly supported by the Spanish MINECO under Project TEC2016-78358-R and Project RTC-2014-1847-6, by the DGA-FSE, by the University of Zaragoza under Project JIUZ-2017-TEC-05, and by the BSH Home Appliances Group.
H. Sarnago, O. Lucía, J.M. Burdío are with the Department of Electronic Engineering and Communications, University of Zaragoza, SPAIN (phone: +34976761000, e-mail: olucia@unizar.es).

This article has been accepted for publication in a future issue of this journal, but has not been fully edited. Content may change prior to final publication. Citation information: DOI 10.1109/TPEL.2018.2815902, IEEE Transactions on Power Electronics

II. POWER CONVERTER TOPOLOGIES FOR FLEXIBLE COOKING SURFACES

Flexible cooking surfaces have been in the last years the most promising domestic induction heating system from a scientific and industrial perspectives [2]. In recent years, several power converters have been proposed, all of them having in common the search of an optimum balance between cost, performance, and control complexity. These converters can be classified according to the base topology from which they are derived, as it is shown in Fig. 2.

Firstly, single-switch class-e inverters [9] have been studied and proposed as a cost-effective implementation which only requires one power device per inductor [10, 11]. However, when implementing multi-coil systems, this approach suffers from severe control limitations due to intermodulation acoustic noise and restrictions in maximum power and soft-switching operation. Consequently, this approach is limited to low power and low inductor number implementations.

The second group is based on the series-resonant half-bridge inverter, which is often considered to have the best balance between cost and performance and, consequently, a sizeable number of converter topologies have been derived from this. In [12], a half-bridge for high-power concentric-inductor domestic IH is proposed. Considering a higher number of coils, [5, 13] proposes a three-device half-bridge structure that achieves a significant cost reduction. [14] focuses on multi-load control, using an intermediate dc-dc converter to provide higher versatility. A different approach is proposed in [6], where different resonant frequencies are set at each coil to perform frequency selection. Finally, in [15-17], the series resonant multi-inverter is proposed as a topology with reduced number of switching devices and versatile control, which is extended to ac-ac operation in [18].

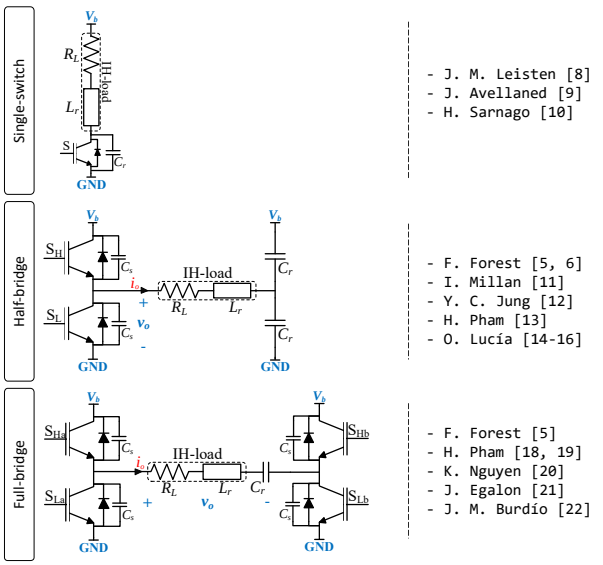

Fig. 2. Basic induction heating topologies used to derive multi-ouput structures.

When higher output power is required, the third family of topologies derived from the full-bridge converter are preferred. In [19-22], the association of multiple full-bridge topologies is proposed to implement a multi-inductor structure, with special considerations to the electromagnetic coupling. These topologies provide higher output power at the cost of a higher device number. In order to provide a cost-effective implementation, in [23] the use of a multiple-output full-bridge topology with a shared half-bridge leg is proposed. Finally, a multiple-output reconfigurable full-bridge is detailed in [5] providing improved versatility.

All the reviewed topologies are derived from classical single-output topologies and have inherent limitations when used as multiple-output converters. This paper proposes a new power converter topology following a matrix structure that allows further optimizing the required number of power devices while providing an accurate and straight-forward control strategy.

III. PROPOSED ZCS MATRIX CONVERTER

A. Converter topology

The proposed multiple-output ZCS resonant inverter is shown in Fig. 3. It is based on a ZCS resonant half-bridge inverter [24] following a matrix approach that enables a significant device reduction while allowing proper output power control. Each load (n,m) is supplied by an upper-side transistor $S_{H,n}$ and lower-side transistor $S_{L,m}$. The upper-side transistors are connected to the dc-link voltage whereas the lower side ones are ground connected. Besides, two additional diodes per load blocks the voltage during the off times and enable independent output power control. By providing the proper activation sequence, it is possible to control the output power in each coil ensuring soft-switching ZCS conditions in the entire output power range and during the full mains cycle. Since the proposed modulation operates below the resonant frequency and no snubber capacitor is used, it is easier to ensure ZCS transitions regardless the output capacitance or operating conditions. This is a significant challenge compared with classical ZVS resonant converters. One of the main benefits of this topology is that in order to implement a N-load appliance, where N is an integer, it requires only an integer switch number $N_{sw}=2N^{1/2}$ plus an integer diode number $N_d=2N$, significantly lower than state-of-the-art implementations. This leads to a significant cost reduction due the the lower number of switching devices and, consequently, PCB size, driving and snubber circuits, digital IOs, etc. Besides, since the proposed topology is fully implemented using fast semiconductors, it enables scanning the cooking area for new pots avoiding the need of an additional pot detection layer, which may significantly increase the cost and complexity of the system.

In order to activate a single induction heating load, it is required to activate the associate upper-side and lower-side transistor in a complementary manner. In Fig. 4, the activation of the induction heating load (i, j) is shown. As it has been previously explained, its associate upper-side transistor and the lower-side transistors, i.e. $S_{H,i}$, $S_{L,j}$, are triggered to activate this load whereas other the remaining

This article has been accepted for publication in a future issue of this journal, but has not been fully edited. Content may change prior to final publication. Citation information: DOI 10.1109/TPEL.2018.2815902, IEEE Transactions on Power Electronics

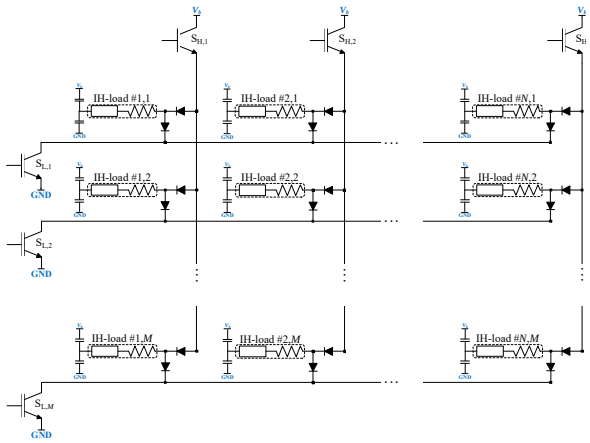

Fig. 3. Proposed multiple-output *N*x*M* ZCS resonant inverter.

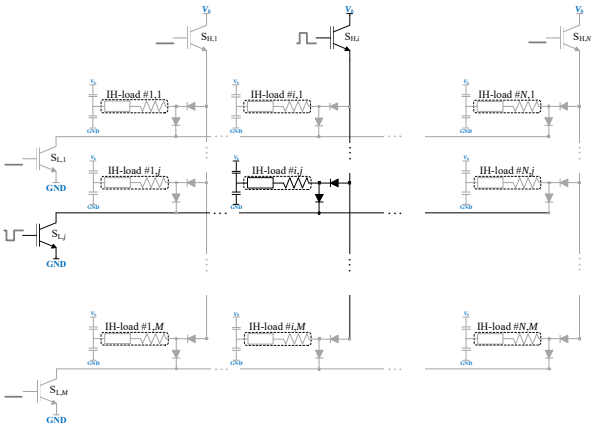

Fig. 4. Single load activation for the induction heating load (*i*, *j*).

transistors, i.e. $S_{H,n}$, $S_{L,m}$, for $n \in \{1..N, n \neq i\}$, $m \in \{1..M, m \neq j\}$, are deactivated. As a result of this, four different scenarios are obtained (Fig. 5):

Case A (Fig. 5(a)): IH(n, m), $n \in \{1..N, n \neq i\}$, $m \in \{1..M, m \neq j\}$, induction heating loads connected to upper-side and lower-side transistors deactivated. In this case, the middle point of the resonant capacitors is set to half the dc-link voltage, v_c=V_b/2 and no current is flowing through these loads, yielding to a zero output power delivered in these loads.

Case B (Fig. 5.b): IH(n, m), $n = i$, $m \in \{1..M, m \neq j\}$, induction heating loads whose upper-side transistor is periodically activated but its lower-side transistor is permanently deactivated. Since a unidirectional path is stablished, the middle point of the resonant capacitors is charged to the dc-link voltage, v_c=V_b, and no current is flowing to the IH load during steady-state condition, leading to a zero output power in these loads.

Case C (Fig. 5(c)): IH(n, m), $n \in \{1..N, n \neq i\}$, $m = j$, induction heating loads whose lower-side transistor are periodically activated whereas its upper-side transistor are permanently deactivated. Since a unidirectional path is stablished, the middle point of the resonant capacitors is ground-connected, v_c=0, and no mean current is flowing to the IH load, leading also to a zero output power in these loads.

Case D (Fig. 5(d)): IH(n, m), $n = i$, $m = j$, induction heating loads whose upper-side and lower-side transistor are periodically activated in a complementary manner. In this case, the induction heating load is energized, being the output power defined by the applied voltage and the induction heating load impedance, as it will be explained in next subsection.

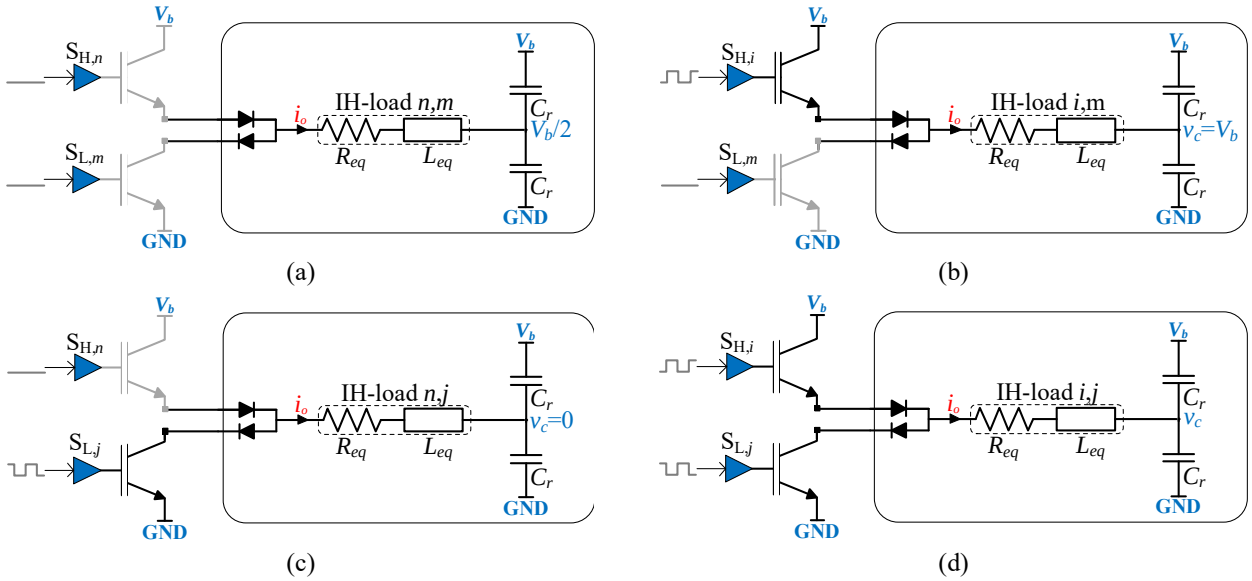

Fig. 5. Different scenarios depending on the asociate upper-side and lower-side activations.

This article has been accepted for publication in a future issue of this journal, but has not been fully edited. Content may change prior to final publication. Citation information: DOI 10.1109/TPEL.2018.2815902, IEEE Transactions on Power Electronics

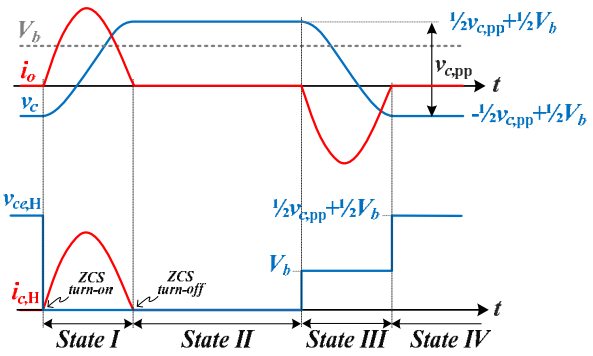

Fig. 6. Main converter waveforms and states. From top to bottom: load current, i_o, resonant capacitor voltage, v_c, upper-side transistor voltage and current, $v_{ce,H}$, $i_{c,H}$, respectively. Equivalent waveforms are expected for the lower-side transitor.

B. *Converter analysis*

The converter analysis is performed for the previously detailed scenario Case D and the main operating waveforms are described in Fig. 6.

During the first state, *State I*, the upper-side transistor $S_{H,i}$, is activated and, therefore, the dc-link voltage is applied to the resonant tank. A resonant current, i_o, starts flowing through the series combination of the upper-side transistor and diode, whereas the resonant capacitor voltage, v_c, charged. This state ends when the resonant current reach the zero level. At this point the series diode blocks the negative current and this path is disconnected. The length of this state is defined by the natural angular frequency associate to the resonant tank, ω_n, being this state duration $t_I=\pi/\omega_n$.

During the second state, *State II*, the resonant tank remains deactivated, blocked by the upper-side series diode. The circuit remains in this state until the lower-side transistor is activated. This state duration is defined by the switching frequency, f_{sw}, and the natural angular frequency, yielding $t_{II}=1/(2f_{sw})-\pi/\omega_n$.

During *State III*, the lower-side transistor is activated, connecting the resonant tank to GND. As a result, the energy stored in the resonant capacitor creates a resonant current flowing through the lower-side series diode and transistor. Again, when the load tries to reach the zero, the resonant tank is open-circuited, resulting the duration of this state is the same as *State I*, $t_{III}=t_I=\pi/\omega_n$, defined by the resonant tank.

Finally, *State IV* is defined by the blank-time where the resonant tank is open-circuited by the lower-side transistor. This state ends when the upper-side transistor is activated. The duration of this state is the same as for the *State II*, $t_{IV}=t_{II}=1/(2f_{sw})-\pi/\omega_n$, if a square wave modulation is considered.

At this point, it is important to note that both during turn-on, i.e. beginning of states I and III, and turn-off, i.e. end of states I and III, zero current switching transition is achieving regardless the operating point. This operation enables the converter to operate in a wide range of switching frequencies with high efficiency, and without

typical constraints in inductive loads regarding snubber capacitors charge.

In order to properly design the converter components and control strategy, it is important to know the coil current, i.e. output current, and the voltage in the resonant capacitor. Considering the series resonant tank, defined by the induction heating load equivalent parameters, i.e. a series resistance, R_{eq}, and a series inductance, L_{eq}, the output current for each load can be defined as

$$i_o(t)=\frac{\hat{V}_{Cr}}{L_{eq}\omega_n}e^{-\xi t}\sin(\omega_n t), \qquad (1)$$

where ξ is defined as $\xi=R_{eq}/2L_{eq}$, and the angular resonant and natural frequencies are $\omega_o=1/\sqrt{L_{eq}C_r}$, $\omega_n=\sqrt{\omega_o^2-\xi^2}$, respectively. The voltage in the resonant capacitor is relevant to select the power device ratings. By applying boundary conditions, the resonant capacitor peak to peak voltage is:

$$v_{c,pp}=\frac{\hat{V}_b}{1-e^{-\xi\frac{\pi}{\omega_n}}}\approx Q_o\hat{V}_b, \qquad (2)$$

where the quality factor for each load is defined as $Q=\omega_o L_{eq}/R_{eq}$. For the proposed topology, the peak voltage in each transistor can be calculated as the peak voltage in resonant capacitor voltage (Fig. 6) as follows

$$\hat{V}_{ce}=\hat{V}_{Cr}=\frac{1}{2}v_{c,pp}+\frac{1}{2}\hat{V}_b\simeq\frac{1}{2}\hat{V}_b(1+Q) \qquad (3)$$

Whereas the diodes only block the same voltage $\hat{V}_{ce}$ minus V_b. Finally, the output power for each load can be calculated as a function of the resonant frequency [24] as follows

$$P_o=f_{sw}\frac{V_{ac,rms}^2}{L_{eq}\omega_o^2}\coth\left(\frac{\pi\xi}{2\omega_n}\right) \qquad (4)$$

From this equation, it is clear that the output power can be easily controlled in each load by linearly modifying the switching frequency. This provide an effective method to control the output power.

It is important to note in order to select the device ratings that each device in a row or column, SL and SH, respectively, must drive all IH loads in that row/column. Consequently, the current ratings of these devices must be adapted according to the number of loads. However, the voltage ratings are the same regardless the number of loads. Moreover, since the diodes are individually connected to each load, the ratings depend only on the desired maximum power per coil.

C. *Modulation strategies*

The input power conversion diagram used in the proposed IH appliance is shown in **¡Error! No se encuentra el origen de la referencia.**. The appliance is supplied from the mains voltage, typically 120/230 V rms, and, afterwards, a full-bridge diode rectifier is used to obtain a high-ripple dc bus. It is important to note that a low value dc-link capacitor is used to ensure a power factor close to one without the need of an additional PFC converter. Consequently, a cost-effective

This article has been accepted for publication in a future issue of this journal, but has not been fully edited. Content may change prior to final publication. Citation information: DOI 10.1109/TPEL.2018.2815902, IEEE Transactions on Power Electronics

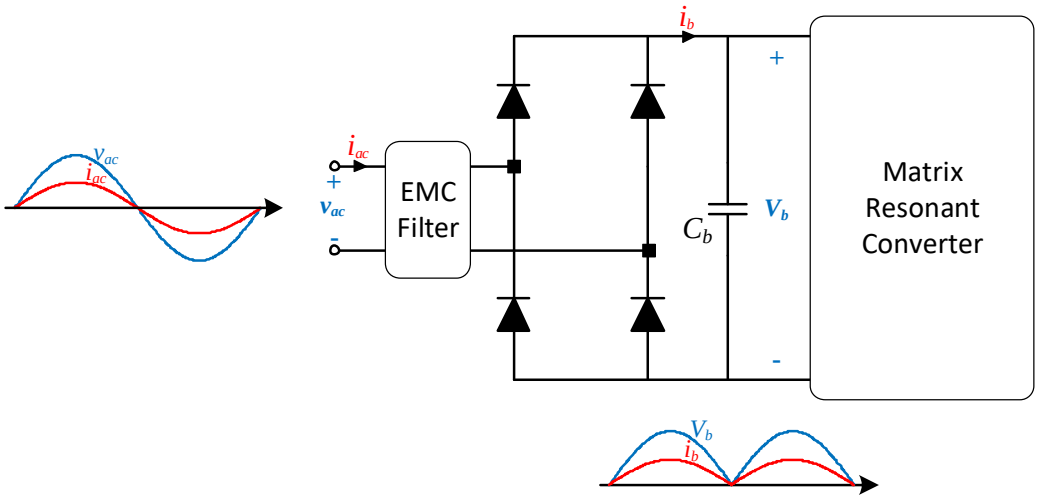

Fig. 7. Detailed ac-dc conversion stage to suply the converter.

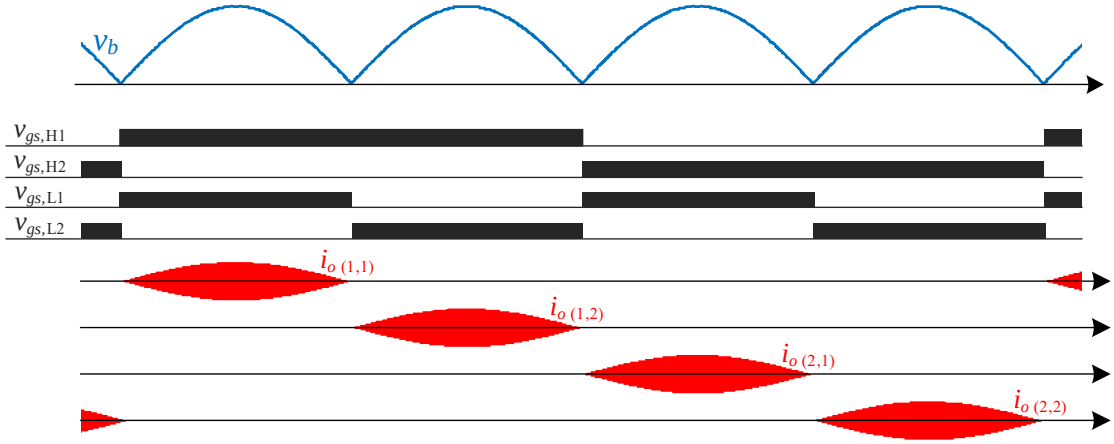

Fig. 8. Main waveforms of the proposed pulse density modulation for a 4-IH load converter.

implementation is obtained and the high-ripple dc bus can be approximated by $v_b=|v_{ac}|$. It is important to note that as a consequence of the amplitude modulation present in the dc bus, all the modulation strategy will be generally synchronized with the mains zero crossing, i.e. each mains half-period.

Two main modulation strategies can be applied to control the output power to each load. Firstly, square wave modulation can be applied to control the output power delivered during each mains half-period, i.e. $p_{(n,\,m),k}$, as a function of the switching frequency applied to the resonant tank, i.e. $f_{sw,k}$.

Secondly, when multiple induction heating loads are activated simultaneously and higher flexibility is required, pulse density modulation (PDM) [25, 26] can be applied, which consist on periodically activating the required coils to achieve the desired mean power $P(n,m)$. When using PDM, during each mains half-period k, the variable $N_{act(n,m),k}=\{0, 1\}$, defines the activation or deactivation of the (n, m) induction heating load, whereas the period of the PDM pattern measured in mains half-cycles is $N_{per,(n,\,m)}$. Therefore, the mean output power delivered to a generic induction heating load results

$$P_{(n,m)} = \frac{1}{N_{per(n,m)}}\left(\sum_{k=1..N_{per,(n,m)}} p_{(n,m),k} N_{\mathrm{act},(n,m),k}\right). \quad (5)$$

An example of the proposed PDM modulation scheme for the case of $N=M=2$, i.e. 4-IH load converter, is shown in Fig. 8. The activation vectors are $\boldsymbol{N_{act(1,\,1)}}=[1, 0, 0, 0]$, $\boldsymbol{N_{act(1,\,2)}}=[0, 1, 0, 0]$, $\boldsymbol{N_{act(2,\,1)}}=[0, 0, 1, 0]$, $\boldsymbol{N_{act(2,\,2)}}=[0, 0, 0, 1]$, whereas the same PDM period is applied to all of them, $N_{per(n,\,m)}=4$. Note that during each activation time, i.e. mains half-cycle, different switching frequencies and, consequently, output power $p_{(n,\,m),k}$ can be applied, leading to an excellent output power control flexibility.

It is important to note that the PDM scheme must be designed to comply with the maximum allowed harmonic and flicker emissions [25] and avoid noticeable power pulsations in the cooking process. Moreover, if it is not properly designed, acoustic noise may also appear due to Lorentz

This article has been accepted for publication in a future issue of this journal, but has not been fully edited. Content may change prior to final publication. Citation information: DOI 10.1109/TPEL.2018.2815902, IEEE Transactions on Power Electronics

forces. However, the proposed topology enables to optimize PDM to arrange pulses to minimize pulsed power and, unlike conventional appliances with great diameter coils, minimize the power pulsed at each small coil.

The proposed topology control strategy must combine square wave modulation and PDM modulation to achieve the desired output power. The output power delivered at each coil is measured and, usually, the same modulation is applied to all coils supplying the same pot, unless there is a significant difference between them. If there is a single pot, only square wave modulation is applied starting at minimum frequency, e.g. 20 kHz, and it is increased until the target output power is achieved for the most restrictive inductor. It is important to note that this is the most common operation scenario. If there are several pots, all the active coils begin also with square wave modulation at minimum frequency, and it is increased until they reach sequentially their target output power. Once each pot reaches its target output power, PDM is applied to maintain the desired output power regardless the frequency imposed by the remaining loads.

IV. EXPERIMENTAL RESULTS

In order to prove the feasibility of this proposal, an experimental prototype has been designed and implemented with 500-W output power per coil. The coils are designed to have 8-cm diameter, leading to inductance values in the range of 150 μH and resistance close to 18 Ω. Besides, the resonant capacitor for each load has been selected to be 22 nF to obtain operating frequencies above the audible range. In order to block the resonant capacitor voltage for any possible condition and enable versatile testing, a 1.6 kV IGBTs have been selected as main transistor whereas a 1.5 kV ULTRA-FAST Diodes have been used in series with the induction heating loads. Fig. 9 shows a render of the experimental prototype PCB.

When dealing with multi-coil IH systems [14, 27, 28], it is important take into account coupling between inductors . In the proposed architecture, the electromagnetic system is designed to minimize coupling [29] by using discrete flux concentrators (Fig. 10). Moreover, heat-diffusing bottom usually placed in most pots, as well as the proposed modulation strategies minimizes any influence on the delivered output power.

The main waveforms for maximum and reduced output power, proving the proper converter operation are shown in Fig. 11. As it can be seen, the output power can be linearly controlled with the switching frequency. The peak voltage is related to the IH load quality factor, yielding up to 600 V peak voltage in the power devices for a 230-Vrms, 50 Hz mains power supply. Moreover, it is important to note that this topology enables real-time pot detection by scanning periodically the complete surface in search of impedance within the IH load range.

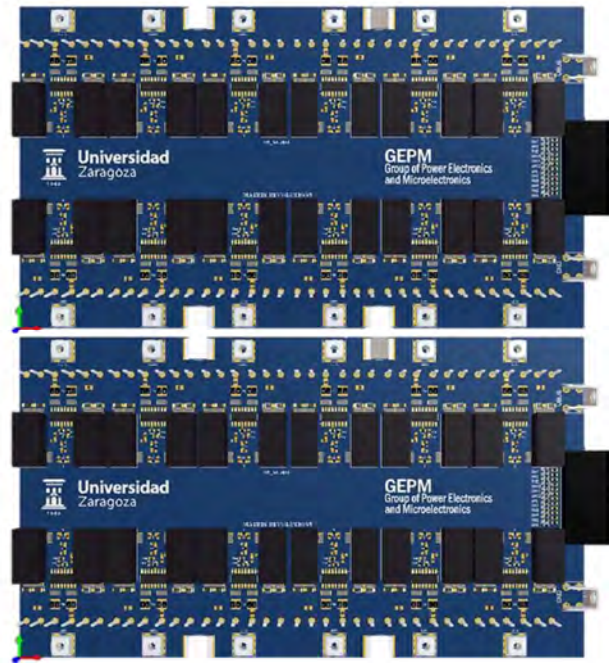

(a)

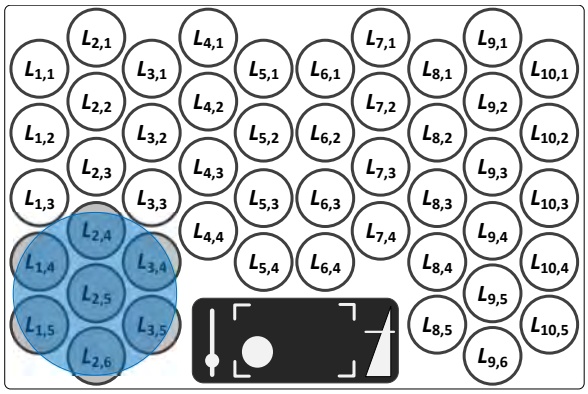

(b)

Fig. 9. Power converter render (a) and $_{example}$ of IH-load placement above the inductor field.

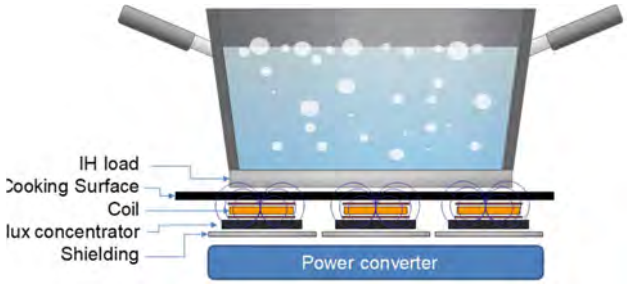

Fig. 10. Implemented multi-coil architecture

This article has been accepted for publication in a future issue of this journal, but has not been fully edited. Content may change prior to final publication. Citation information: DOI 10.1109/TPEL.2018.2815902, IEEE Transactions on Power Electronics

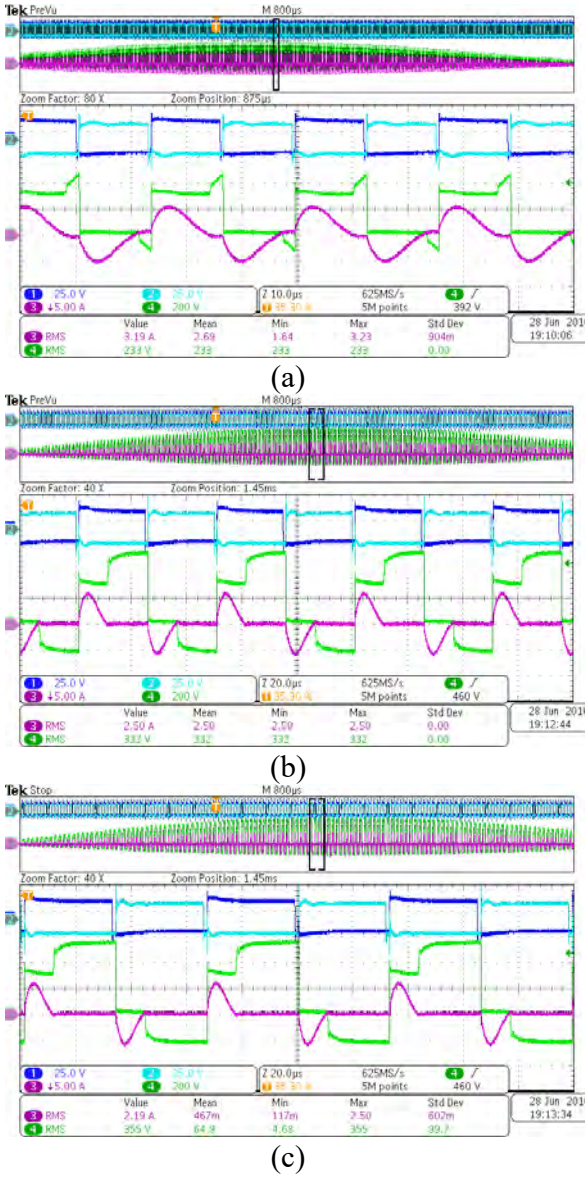

Fig. 11. Main waveforms in a coil i,j during a mains half-period for maximum (a) and reduced $_{output}$ power (b,c). From top to bottom: control signals SH,j and SL,I (25 V/div), transistor blocking voltage (200 V/div) and coil current (5 A/div).

Fig. 12 shows the main converter waveforms including the control signals and curren through the coils for a 4-IH load configuration operating with PDM modulation. In this figure and zoomed detail, the correct converter operation can be seen as well as the versatility of PDM control.

Finally, Fig. 13 shows different PDM activation patterns featuring different number of active cycles as well as different power distribution among the IH loads. These experimental results prove the proper converter operation of the proposed matrix ZCS converter and its control strategy for multi-load management, making this proposal a solid and cost-effective system for flexible cooking surfaces.

V. DISCUSSION

Flexible cooking surfaces are the future of domestic induction heating. Nowadays, two main approaches are followed: the use of multiple inverter-coil pairs and the use of a one or several high-power inverters (Implementation I) and electromechanical relays to select the desired coils to be activated (Implementation II). The former solution usually achieves higher performance at a higher cost, whereas the latter reduces the number of power devices reducing its performance. The power converter proposed in this paper, however, achieves an excellent balance between performance and cost, tangible by analyzing several key elements (Table I): component count, output power control, IH load detection, and efficiency.

Implementation I, following the classical inverter-coil approach, requires clearly the highest device count, leading to a costly implementation. Moreover, the semiconductor usage ratio of this approach is very low, resulting in a poor utilization of the available devices, and due to switching frequencies restriction due to acoustic noise, having a higher number of inverters do not imply higher control versatility. For these reasons, this approach is usually not feasible when N is high, typical of flexible cooking surfaces. Implementation II decreases significantly the number of required devices, being typically determined by the number of k independent inverters available, i.e. independent IH loads. However, this approach requires an electromechanical relay array with more than N devices which also adds

TABLE I
RESONANT INVERTER TOPOLOGY COMPARISON FOR AN N-COIL IMPLEMENTATION

	DEVICE COUNT			POWER CONTROL	LOAD DETECTION	EFFICIENCY
	Transistors	Diodes	EM Relays			
Implementation I: Multiple inverter-coil cells	$2N$	$2N$	0	Best	Real time	Best
Implementation II: Single inverter plus relay array	$2k$ (k<<N)	$2k$ (k<<N)	>N	Poor	Additional layer	Poor
Proposed ZCS Matrix Resonant inverter	$2N^{1/2}$	$2N$	0	Better	Real time	Better

This article has been accepted for publication in a future issue of this journal, but has not been fully edited. Content may change prior to final publication. Citation information: DOI 10.1109/TPEL.2018.2815902, IEEE Transactions on Power Electronics

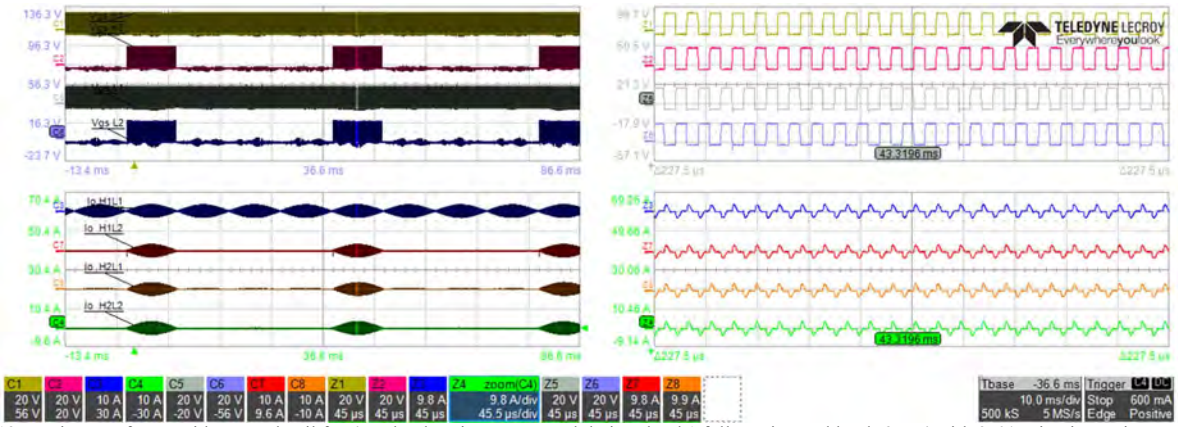

Fig. 12. Main waveforms with zoom detail for 4 IH loads using PDM modulation: load 1 fully active and loads 2 to 4 with 25% acivation ration. From top to bottom: control signals (20 V/div) and coil currents (10 A/div). Time: 10 ms/div (left) and 45 µs/div (right).

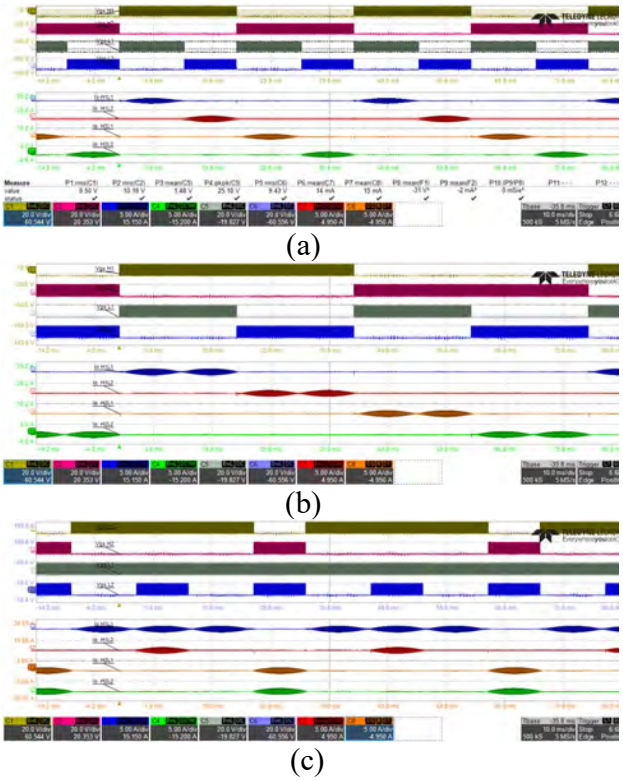

Fig. 13. Main waveforms with zoom detail for 4 IH loads using PDM modulation with $_{\text{differnet}}$ patterns. From top to bottom: control signals (20 V/div) and coil currents (10 A/div). Time: 10 ms/div (left) and 45 µs/div (right).

acoustic noise, complexity, and cost. It is important to note that Implementation II also requires an additional load detection layer and suffers from poor power control due to the limited inverter number and EM relays. The proposed approach, however, reduces the number of devices of Implementation I without degrading the performance as it occurs with implementation II. Moreover, the proposed

topology allows the use of several matrices and/or vectors to maximize the control possibilities.

Finally, efficiency has a direct impact in the energy consumption and environmental impact, as well as the thermal performance of the devices. Implementation I achieves the same high efficiency of the classical half-bridge series resonant implementation, whereas Implementation II suffers from control issues that leads to operation far from the resonant point and complex snubber network design that

undermines the final efficiency. The proposed implementation has an additional series diode in the current path. However, the operation with very low switching frequency and the use of pulse density modulation can compensate the additional losses. Consequently, the proposed ZCS matrix resonant inverter achieves a cost-effective execution with a well-balanced performance, providing an excellent implementation for flexible cooking surfaces.

VI. CONCLUSIONS

Flexible cooking surfaces are one of the most innovative appliances providing the user with superior performance and flexibility. However, significant challenges remains to design a power electronic converter to implement such system in an efficient and cost-effective way. To achieve this aim, in this paper a multiple-output ZCS resonant inverter for multi-coil induction heating systems has been proposed. The proposed converter enables high performance operation, soft-switching and accurate output power control regardless the operating conditions. Moreover, the proposed topology follows a matrix-based architecture that significantly reduces the number of required switches for appliances with a high number of coils, leading to a cost-effective implementation. In order to prove the feasibility of this proposal, an experimental prototype has been designed and built, providing 500-W output power per load. The proper soft-switching operation as well as the proposed pulse density modulation control strategies have been tested, showing the expected performance and validating the benefits of this proposal. As a conclusion, the proposed multiple-output ZCS

resonant inverter is proposed as a high-performance, versatile, and cost-effective approach to implement flexible cooking surfaces.

REFERENCES

[1] V. Esteve *et al.*, "Improving the reliability of series resonant inverters for induction heating applications," *IEEE Transactions on Industrial Electronics,* vol. 61, no. 5, pp. 2564-2572, May 2014.

[2] O. Lucía, J. Acero, C. Carretero, and J. M. Burdío, "Induction heating appliances: Towards more flexible cooking surfaces," *IEEE Industrial Electronics Magazine,* vol. 7, no. 3, pp. 35-47, September 2013.

[3] P. Di Barba, F. Dughiero, E. Sieni, and A. Candeo, "Coupled field synthesis in magnetic fluid hyperthermia," *IEEE Transactions on Magnetics,* vol. 47, no. 5, pp. 914-917, May 2011.

[4] O. Lucía, P. Maussion, E. Dede, and J. M. Burdío, "Induction heating technology and its applications: Past developments, current technology, and future challenges," *IEEE Transactions on Industrial Electronics,* vol. 61, no. 5, pp. 2509-2520, May 2014.

[5] F. Forest, S. Faucher, J.-Y. Gaspard, D. Montloup, J.-J. Huselstein, and C. Joubert, "Frequency-synchronized resonant converters for the supply of multiwindings coils in induction cooking appliances," *IEEE Transactions on Industrial Electronics,* vol. 54, no. 1, pp. 441-452, February 2007.

[6] F. Forest, E. Labouré, F. Costa, and J.-Y. Gaspard, "Principle of a multi-load/single converter system for low power induction heating," *IEEE Transactions on Industrial Electronics,* vol. 15, no. 2, pp. 223-230, March 2000.

[7] C. Carretero, R. Alonso, and J. Acero, "Interference Emission Estimation of Domestic Induction Cookers Based on Finite-Element Simulation," *IEEE Transactions on Electromagnetic Compatibility,* vol. 58, no. 4, pp. 993-999, 2016.

[8] H. Sarnago, O. Lucía, and J. M. Burdío, "Multiple-output ZCS resonant inverter for multi-coil induction heating appliances," in *IEEE Applied Power Electronics Conference and Exposition*, 2017, pp. 2234-2238.

[9] J. M. Leisten, A. K. Lefedjiev, and L. Hobson, "Single ended resonant power supply for induction heating," *Electronics Letters,* vol. 26, no. 12, pp. 814-816, December 1990.

[10] J. Avellaned, C. Bernal, and P. Molina, "SiC multi-inverter frequency band division design for increased flexibility in an induction heating surface area," in *2013 15th European Conference on Power Electronics and Applications (EPE)*, 2013, pp. 1-5.

[11] H. Sarnago, O. Lucia, A. Mediano, and J. M. Burdio, "A Class-E Direct AC-AC Converter With Multicycle Modulation for Induction Heating Systems," *IEEE Transactions on Industrial Electronics,* vol. 61, no. 5, pp. 2521-2530, May 2014.

[12] I. Millán, J. M. Burdío, J. Acero, O. Lucía, and D. Palacios, "Resonant inverter topologies for three concentric planar windings applied to domestic induction heating," *Electronics Letters,* vol. 46, no. 17, pp. 1225-1226, 2010.

[13] Y.-C. Jung, "Dual half bridge series resonant inverter for induction heating appliance with two loads," *Electronics Letters,* vol. 35, no. 16, pp. 1345-1346, May 1999.

[14] H. Pham, H. Fujita, K. Ozaki, and N. Uchida, "Phase angle control of high-frequency resonant currents in a multiple inverter system for zone-control induction heating," *IEEE Transactions on Power Electronics,* vol. 26, no. 11, pp. 3357-3366, 2011.

[15] O. Lucía, J. M. Burdío, L. A. Barragán, J. Acero, and I. Millán, "Series-resonant multiinverter for multiple induction heaters," *IEEE Transactions on Power Electronics,* vol. 24, no. 11, pp. 2860-2868, November 2010.

[16] O. Lucía, J. M. Burdío, L. A. Barragán, J. Acero, and C. Carretero, "Series resonant multi-inverter with discontinuous-mode control for improved light-load operation," *IEEE Transactions on Industrial Electronics,* vol. 58, no. 11, pp. 5163-5171, November 2011.

[17] O. Lucía, H. Sarnago, and J. M. Burdío, "Soft-Stop Optimal Trajectory Control for Improved Performance of the Series Resonant Multi-Inverter for Domestic Induction Heating Applications," *IEEE Transactions on Industrial Electronics,* vol. 62, no. 10, pp. 6251-6259, October 2015.

[18] O. Lucía, C. Carretero, J. M. Burdío, J. Acero, and F. Almazán, "Multiple-output resonant matrix converter for multiple induction heaters," *IEEE Transactions on Industry Applications,* vol. 48, no. 4, pp. 1387-1396, July/August 2012.

[19] H. Pham, H. Fujita, K. Ozaki, and N. Uchida, "Dynamic analysis and control of a zone-control induction heating system," in *IEEE Energy Conversion Congress and Exposition (ECCE)*, 2011, pp. 4093-4100.

[20] H. N. Pham, H. Fujita, K. Ozaki, and N. Uchida, "Dynamic analysis and control for resonant currents in a zone-control induction heating system," *IEEE Transactions on Power Electronics,* vol. 28, no. 3, pp. 1297-1307, March 2013.

[21] K. Nguyen, O. Pateau, S. Caux, and P. Maussion, "Robustness of a resonant controller for a multiphase induction heating system," *IEEE Transactions on Industry Applications,* vol. 51, no. 1, pp. 73-81, Jan./Feb. 2014.

[22] J. Egalon, S. Caux, P. Maussion, M. Souley, and O. Pateau, "Multiphase system for metal disc induction heating: Modeling and RMS current control," *IEEE Transactions on Industry Applications,* vol. 48, no. 5, pp. 1692-1699, September/October 2012.

[23] J. M. Burdío, F. Monterde, J. R. García, L. A. Barragán, and A. Martínez, "A two-output series-resonant inverter for induction-heating cooking appliances," *IEEE Transactions on Power Electronics,* vol. 20, no. 4, pp. 815-822, July 2005.

[24] H. Sarnago, O. Lucia, A. Mediano, and J. Burdio, "Efficient and cost-effective ZCS direct ac-ac resonant converter for induction heating," *IEEE Transactions on Industrial Electronics,* vol. 61, no. 5, pp. 2546-2555, May 2014.

[25] O. Lucía, J. M. Burdío, I. Millán, J. Acero, and D. Puyal, "Load-adaptive control algorithm of half-bridge series resonant inverter for domestic induction heating," *IEEE Transactions on Industrial Electronics,* vol. 56, no. 8, pp. 3106-3116, August 2009.

[26] H. Fujita and H. Akagi, "Pulse-density-modulated power control of a 4 kW, 450 kHz voltage-source inverter for induction melting applications," *IEEE Transactions on Industry Applications,* vol. 32, no. 2, pp. 279-286, March/April 1996.

[27] M. Souley, S. Caux, J. Egalon, O. Pateau, Y. Lefevre, and P. Maussion, "Optimization of the settings of multiphase induction heating system," *IEEE Transactions on Industry Applications,* vol. 49, no. 6, pp. 2444-2450, 2013.

[28] C. Carretero, O. Lucía, J. Acero, and J. M. Burdío, "Computational modeling of two partly-coupled coils supplied by a double half-bridge resonant inverter for induction heating appliances," *IEEE Transactions on Industrial Electronics,* vol. 60, no. 8, pp. 3092-3105, August 2013.

[29] C. Carretero, J. Acero, R. Alonso, J. M. Burdio, and F. Monterde, "Modeling Mutual Impedances of Loaded Non-Coaxial Inductors for Induction Heating Applications," *IEEE Transactions on Magnetics,* vol. 44, no. 11, pp. 4115-4118, 2008.

This article has been accepted for publication in a future issue of this journal, but has not been fully edited. Content may change prior to final publication. Citation information: DOI 10.1109/TPEL.2018.2815902, IEEE Transactions on Power Electronics

Hector Sarnago (S'09 M'15) received the M.Sc. degree in Electrical Engineering and the Ph.D. degree in Power Electronics from the University of Zaragoza, Spain, in 2010 and 2013, respectively. Currently, he is a senior post-doc researcher in the the Department of Electronic Engineering and Communications at the University of Zaragoza, Spain. His main research interests include resonant converters and digital control for induction heating applications.
Mr. Sarnago is a member of the Aragon Institute for Engineering Research (I3A).

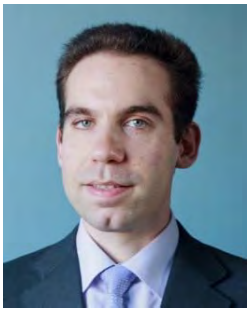

Óscar Lucía (S'04, M'11, SM'14) received the M.Sc. and Ph.D. degrees (with honors) in Electrical Engineering from the University of Zaragoza, Spain, in 2006 and 2010, respectively.
He is an assistant professor at the University of Zaragoza. His main research interests include resonant power conversion, wide-bandgap devices, and digital control, mainly applied to contactless energy transfer, induction heating, and biomedical applications. In these topics, he has published more than 50 international journal papers and 100 conference papers, and he has filed more than 25 patents.
Dr. Lucía is a Senior Member of the IEEE and an active member of the Power Electronics (PELS) and Industrial Electronics (IES) societies. Currently, he is an Associate Editor of the *IEEE Transactions on Industrial Electronics* and *IEEE Transactions on Power Electronics*. Dr. Lucía is a member of the Aragon Institute for Engineering Research (I3A).

José M. Burdío (M'97–SM'12) received the M.Sc. and Ph.D. degrees in electrical engineering from the University of Zaragoza, Zaragoza, Spain, in 1991 and 1995, respectively.
He has been with the Department of Electronic Engineering and Communications, University of Zaragoza, where he is currently a Professor, the Head of the Group of Power Electronics and Microelectronics, and the Director of the BSH Power Electronics Laboratory at the University of Zaragoza. During 2000 he was a visiting professor at the Center for Power Electronics Systems, Virginia Tech. He is the author of more than 80 international journal papers and over 200 papers in conference proceedings and the holder of more than 60 international patents. His main research interests include modeling of switching converters and resonant power conversion for induction heating and biomedical applications.
Dr. Burdío is a senior member of the IEEE and the Power Electronics and Industrial Electronics Societies.